TRENDS IN SCIENCES 2026; 23(5): 12285
https://doi.org/10.48048/tis.2026.12285 RESEARCH ARTICLE

Glycyrrhizic Acid Monoammonium Complex (XF-2): Chemical Profile and Immunomodulatory Evaluation

Fayyoza Khurramova[1,*], Rakhmat Esanov[1,2], Izzatullo Abdullaev[1], Ulugbek Gayibov[1], Kuralbay Rezhepov[1] and Alimjon Matchanov[1]

[1]*A.S. Sadykov Institute of Bioorganic Chemistry of the Science Academy of Uzbekistan, Tashkent, Uzbekistan*
[2]*National University of Uzbekistan, Tashkent, Uzbekistan*

([*]Corresponding author's e-mail: khurramova1988@mail.ru)

Received: 15 October 2025, Revised: 22 October 2025, Accepted: 29 October 2025, Published: 20 January 2026

Abstract

This study explores the physicochemical and biological properties of the supramolecular complex XF-2, composed of glycyrrhizic acid monoammonium salt and anti-tuberculosis drugs pyrazinamide, isoniazid, rifampicin, and levofloxacin. UV-Vis spectroscopy revealed a bathochromic shift from 254 to 264 nm, confirming electronic interactions between glycyrrhizic acid and the guest molecules. FTIR spectra showed characteristic bands at 1,658 cm^{-1} (C=O) and 1,593 cm^{-1} ($–COO^-$), indicating ionic and hydrogen-bonded interactions responsible for supramolecular assembly formation. Molecular docking analysis demonstrated stable binding of XF-2 components with NF-κB p52 (2AZ5), IL-10 (1VLK), and IL-6 receptor (1A3Q), with binding energies ranging from –4.6 to –9.2 kcal/mol. Rifampicin and levofloxacin exhibited the strongest affinities, forming multiple hydrogen bonds, π-π stacking, and electrostatic interactions with key amino acid residues. In vivo studies showed that XF-2 is low-toxic (LD_{50} = 4,050 mg/kg) and exerts marked immunomodulatory activity in prednisolone-induced immunosuppressed mice. At 1,000 mg/kg, the complex significantly increased thymus and spleen indices, restoring immune organ weights close to normal values. Together, spectroscopic, computational, and pharmacological data confirm that XF-2 is a stable, safe, and biologically active supramolecular formulation with strong immunorestorative potential, making it a promising candidate for further development as an immunomodulatory and protective agent.

Keywords: Glycyrrhizic acid monoammonium salt, Supramolecular complex, UV-Vis and FTIR spectroscopy, Molecular docking, NF-κB p52, Immunomodulatory activity, Low toxicity, Prednisolone-induced immunosuppression

Introduction

Glycyrrhizic acid (GA) and its monoammonium salts (GAM) have attracted growing attention as natural amphiphilic molecules capable of forming supramolecular complexes with various pharmacologically active substances [1-3]. Due to their unique structural properties—hydrophilic glucuronic residues and a hydrophobic glycyrrhetinic aglycone—these compounds can self-assemble into micellar or inclusion-type systems that enhance drug solubility, stability, and membrane permeability [4-6].

In addition to its carrier functions, GA itself exhibits pronounced anti-inflammatory and immunomodulatory effects. It has been shown to modulate the activity of macrophages, T-lymphocytes, and dendritic cells, as well as regulate the production of cytokines such as IL-2, IL-6, and TNF-α [6-9]. These mechanisms are crucial for maintaining immune homeostasis during infectious and inflammatory processes.

Based on these pharmacological and structural advantages, GA and GAM have been proposed as molecular carriers and immunomodulatory enhancers in

the design of multi-component drug systems [9,10]. One of the most promising approaches involves combining GAM with classical anti-tuberculosis agents to improve their bioavailability and safety profiles while simultaneously potentiating immune function.

In the present work, we investigated the glycyrrhizic acid monoammonium supramolecular complex (XF-2) containing four first-line and second-line anti-tuberculosis drugs—isoniazid, rifampicin, pyrazinamide, and levofloxacin. The study aimed to characterize the chemical structure and molecular interactions of XF-2 using UV-Vis and FTIR spectroscopy and to explore its binding affinities with key immunomodulatory proteins (IL-2, IL-6 receptor, TNF-α) through molecular docking [11-13]. Furthermore, in vivo experiments were conducted to assess the acute toxicity and immunomodulatory potential of the complex in experimental animals.

Collectively, this multidisciplinary study provides new insights into the chemical and biological behavior of the glycyrrhizic acid monoammonium complex XF-2, suggesting that such supramolecular systems may serve as low-toxic immunoprotective platforms for enhancing the efficacy of anti-tuberculosis therapy [14-16].

Materials and methods

Animal ethics

All preoperative and experimental procedures were carefully reviewed and approved by the Institutional Committee for Animal Use and Care. The animals were housed in a vivarium under standardized conditions, including a relative humidity of 55% - 65%, a controlled ambient temperature of 22 ± 2 °C, and unrestricted access to water and standard laboratory chow. All aspects of animal care and handling were conducted in full compliance with the European Directive 2010/63/EU, which governs the protection of animals used for scientific research. Ethical clearance for this study was granted by the Animal Ethics Committee of the Institute of Bioorganic Chemistry, Academy of Sciences of the Republic of Uzbekistan (Protocol No. 133/1a/h, dated 4 August 2016).

Preparation of supramolecular complexes

Supramolecular complexes of glycyrrhizic acid (GA) and its monoammonium salt (GAM) with first-line and second-line anti-tuberculosis drugs were obtained through gradual molecular assembly. The active components—isoniazid, rifampicin, pyrazinamide, lomefloxacin, and levofloxacin—were combined with GA or GAM in aqueous or hydroalcoholic medium under mild stirring conditions (25 ± 2 °C). GA or GAM was first dissolved in distilled water, after which drug solutions were added dropwise with continuous mixing until a transparent or slightly opalescent system was formed. The resulting mixture was kept at 4 °C for 24 h to allow self-organization of the supramolecular structure, filtered through a 0.22 μm membrane, and stored for subsequent analyses. The complex investigated in this study, XF-2, consisted of the monoammonium salt of GA with isoniazid, rifampicin, pyrazinamide, and levofloxacin [17,18].

UV-Visible Spectroscopy

The optical characteristics of the XF-2 complex were studied using a UV-visible spectrophotometer in the range of 200 - 400 nm with 1 cm quartz cuvettes. Individual component spectra (GA, GAM, and each drug) and the spectrum of the complex were compared. Bathochromic or hypsochromic shifts of λ_max and changes in absorption intensity were interpreted as evidence of molecular interaction and complex formation. The presence of isosbestic points indicated the establishment of stable supramolecular equilibria [19,20].

Fourier Transform Infrared (FTIR) spectroscopy

Infrared spectra were recorded in the 4,000 - 400 cm^{-1} range using the ATR technique with 4 cm^{-1} resolution. The spectra of free GA/GAM, individual drugs, and the XF-2 complex were compared to identify changes in the vibrational frequencies of key functional groups (–OH, –COOH, C=O, N–H). Shifts in the carbonyl and hydroxyl stretching bands and broadening of absorption regions were interpreted as the formation of hydrogen-bonded and ionic associations within the supramolecular structure [21,22].

Acute toxicity study

Acute toxicity of the XF-2 complex was assessed according to the Litchfield and Wilcoxon method on healthy white mice of both sexes weighing 18 - 22 g.

The animals were quarantined for 10 - 14 days prior to testing and divided into six experimental groups of six mice each. XF-2 was administered orally as an 8.1% suspension at doses of 2,025, 2,835, 3,645, 4,455, 5265, and 5,670 mg/kg. Since the maximum peroral volume was limited to 0.5 mL/20 g, larger doses were given fractionally with 10-minute intervals between portions. Animals were observed for 14 days to monitor clinical signs and mortality, and the median lethal dose (LD_{50}) was calculated with 95% confidence limits [23].

Immunomodulatory activity

The immunomodulatory potential of XF-2 was investigated using a prednisolone-induced immunosuppression model. White mice weighing 19 - 24 g were divided into groups of 6 animals each. Immunosuppression was induced by intramuscular administration of prednisolone at a dose of 150 mg/kg (1.5 % solution, 0.2 mL/20 g) once daily for 6 consecutive days. The experimental groups received XF-2 orally 1 h prior to prednisolone injection at doses of 500, 1,000, and 1,500 mg/kg, while the control group received prednisolone only [24].

Molecular docking: Software and databases

Molecular docking studies were performed to evaluate the interaction of bioactive components of the glycyrrhizic acid monoammonium complex (XF-2) with key immunomodulatory proteins. The crystallographic structures of interleukin-2 (IL-2, PDB ID: 1VLK), tumor necrosis factor-α (TNF-α, PDB ID: 2AZ5), and the interleukin-6 receptor (IL-6R, PDB ID: 1A3Q) were retrieved from the Protein Data Bank (PDB). Ligand structures of isoniazid, rifampicin, pyrazinamide, and levofloxacin were obtained from the PubChem database and converted into PDBQT format using AutoDock Tools (ADT). Docking simulations were carried out in AutoDock 4.2 employing the Lamarckian Genetic Algorithm to predict the optimal ligand-protein binding conformations. The docked complexes were visualized and analyzed using PyMOL and Discovery Studio Visualizer 2023, allowing identification of hydrogen bonds, hydrophobic contacts, and key amino acid residues responsible for complex stabilization. This computational approach provided insight into the binding affinity and potential immunomodulatory mechanisms of the XF-2 supramolecular system [25].

Data analysis and statistics

All experimental data were processed and analyzed using OriginPro 9.0 (OriginLab Corporation, USA). Quantitative results are expressed as the mean ± standard error of the mean (SEM), based on data obtained from at least six animals per group (n = 6). The relative organ weight coefficients of the thymus and spleen were calculated to assess the immunomodulatory effects of the XF-2 complex. Statistical evaluation was performed using 1-way analysis of variance (ANOVA) followed by Tukey's post hoc test to determine intergroup differences. When the data did not meet the criteria for normal distribution, the Kruskal-Wallis test was applied. A difference was considered statistically significant at $p < 0.05$.

Results and discussion

Formation and physicochemical characterization of supramolecular complexes

The supramolecular complexes of glycyrrhizic acid (GA) and its monoammonium salt (GAM) with anti-tuberculosis agents—isoniazid, rifampicin, pyrazinamide, lomefloxacin, and levofloxacin—were synthesized through self-assembly of low-molecular-weight amphiphilic components. The general scheme of complex formation is presented in **Figure 1**. In this process, the hydrophilic glucuronic residues and hydrophobic triterpenoid aglycone of GA (or GAM) interact with the functional groups of drug molecules through hydrogen bonding, electrostatic attraction, and van der Waals forces, forming thermodynamically stable supramolecular aggregates. The resulting systems can be regarded as host-guest type complexes, in which GA or GAM acts as a supramolecular carrier for the incorporated drugs. Depending on the molar ratio (n = 4.6; x = 0.5 - 5), different degrees of molecular association were obtained, leading to the formation of stable, water-dispersible complexes suitable for further physicochemical analysis [26].

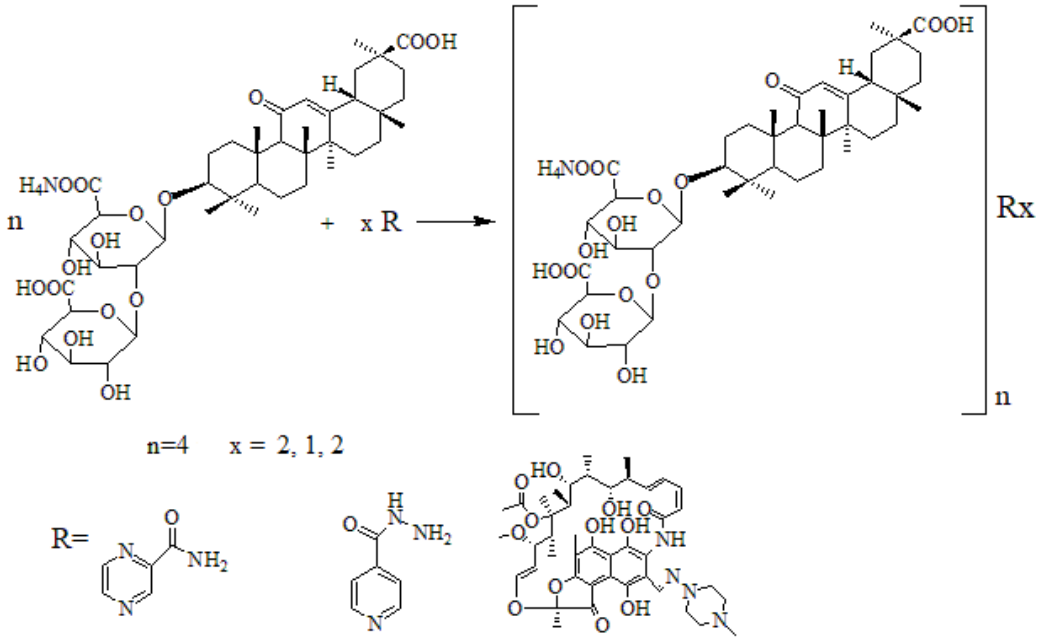

Figure 1 General scheme of supramolecular complex formation between glycyrrhizic acid (GA) or its monoammonium salt (GAM) and anti-tuberculosis agents.

To evaluate the hydrodynamic behavior of these supramolecular assemblies, the reduced viscosity of the GAM-pyrazinamide-isoniazid complex in a 4:2:1 ratio was measured at various concentrations (**Figure 2**). The reduced viscosity increased gradually with concentration, indicating the presence of concentration-dependent molecular association and aggregation in aqueous solution at 25 °C. This pattern is consistent with the self-organization behavior of amphiphilic molecules, where intermolecular hydrogen bonding and hydrophobic interactions contribute to network formation. The influence of the medium on complex viscosity was further examined in the presence of urea, xylose, and potassium chloride (KCl). Urea, known to disrupt hydrogen bonds, significantly decreased viscosity, while xylose, which screens hydrophobic interactions, and KCl, which alters ionic strength, produced moderate changes (**Figure 3**). These findings confirm that both hydrogen bonding and hydrophobic interactions play crucial roles in maintaining the structural integrity of the complexes. Temperature-dependent measurements of a 0.1% aqueous solution of the complex revealed a gradual decrease in reduced viscosity between 25 and 35 °C, followed by a sharp drop from 35 to 40 °C, and a slower decline up to 45 °C (**Figure 4**). This temperature sensitivity suggests partial disruption of non-covalent interactions, accompanied by rearrangement of orientation forces between polar regions of the molecules. The resulting changes in micellar volume and fluidity reflect the dynamic nature of supramolecular interactions within the GAM-based complexes. Although composed of low-molecular-weight components, the viscosity behavior of these systems resembles that of polymeric solutions. This can be attributed to the formation of transient supramolecular networks stabilized by multiple non-covalent forces, whose structural organization and flow properties are responsive to both concentration and temperature. Such behavior provides further evidence for the formation of cooperative, self-assembled supramolecular architectures in the glycyrrhizic acid monoammonium systems [27].

UV-Vis spectral analysis

The UV-visible spectra of glycyrrhizic acid (GA), pyrazinamide, isoniazid, and their supramolecular complex GA:pyrazinamide:isoniazid (4:2:1) were recorded in aqueous medium (**Figure 2**). Distinct absorption maxima characteristic of each component were observed. The spectrum of isoniazid showed an absorption maximum at 265 nm, corresponding to n → π* electronic transitions of the amide group [28,29].

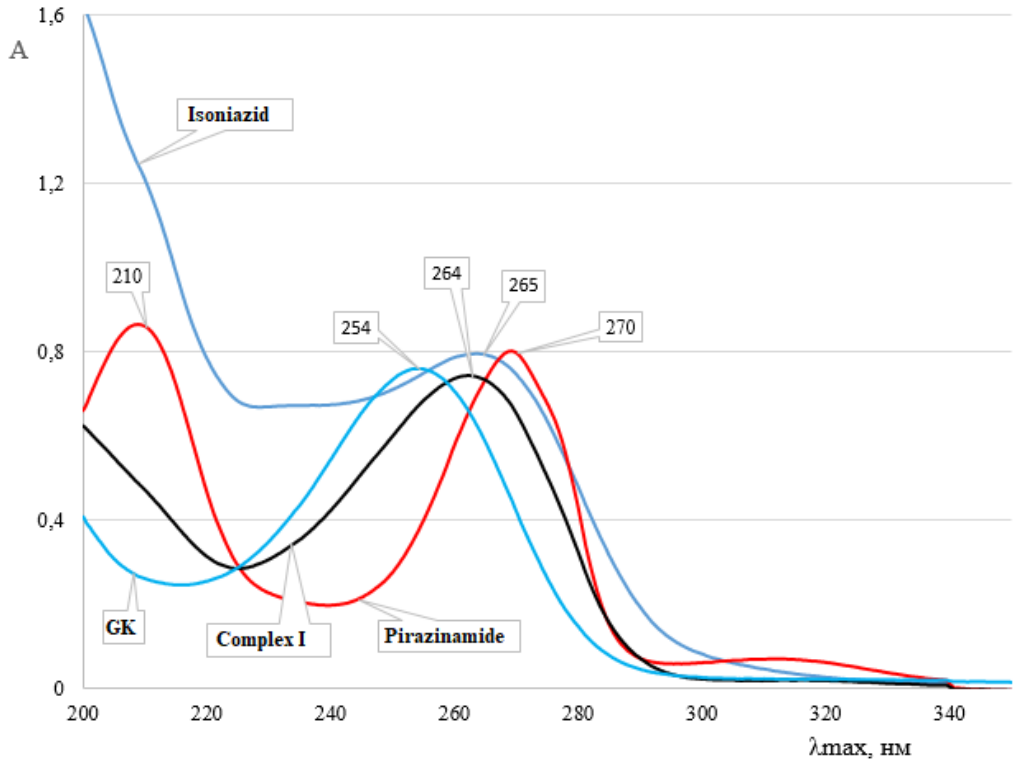

Figure 2 UV-Vis spectra of glycyrrhizic acid (GA), pyrazinamide, isoniazid, and the supramolecular complex GA:pyrazinamide:isoniazid (4:2:1) in aqueous solution. The complex exhibits a bathochromic shift of the absorption maximum to 264 nm, confirming molecular association through hydrogen bonding and orbital overlap.

The pyrazinamide molecule exhibited 2 well-defined absorption bands: one at 210 nm attributed to π → π* transitions within the pyridine ring, and another at 270 nm due to n → π* transitions of the amide carbonyl group. The spectrum of glycyrrhizic acid displayed a single absorption maximum at 254 nm, typical of n → π* transitions associated with the carbonyl chromophore of the triterpenoid structure. Upon complexation, the resulting GA:pyrazinamide:isoniazid (4:2:1) system exhibited a broadened absorption band with a slight bathochromic shift to 264 nm, indicating a modification in the electronic environment of the GA chromophore. This spectral shift confirms the formation of a supramolecular complex through non-covalent interactions, primarily hydrogen bonding and dipole–dipole coupling between GA and the incorporated drug molecules. The bathochromic displacement suggests a redistribution of electron density within the molecular orbitals, which can be attributed to the participation of non-bonding electron pairs from the ligand molecules in intermolecular orbital interactions.

FTIR spectral analysis

The FTIR spectrum of the supramolecular complex GAM:pyrazinamide:isoniazid (4:2:1) is presented in **Figure 3**. The characteristic absorption band of the C=O stretching vibration in the aglycone moiety of glycyrrhizic acid monoammonium salt (GAM) was observed at 1,658 cm^{-1}, corresponding to the carbonyl group at the C-11 position of the triterpenoid skeleton. In addition, the carboxylate group vibrations of the GAM molecule appeared at 1,593 cm^{-1}, which showed a noticeable increase in intensity in the complex spectrum compared with the spectrum of the free GAM. This enhancement indicates the involvement of electrostatic interactions between the deprotonated carboxyl groups of GAM ($–COO^-$) and the protonated amino groups of the drug molecules ($–NH_3^+$), confirming the formation of ionic hydrogen-bonded associations within the supramolecular structure [30,31].

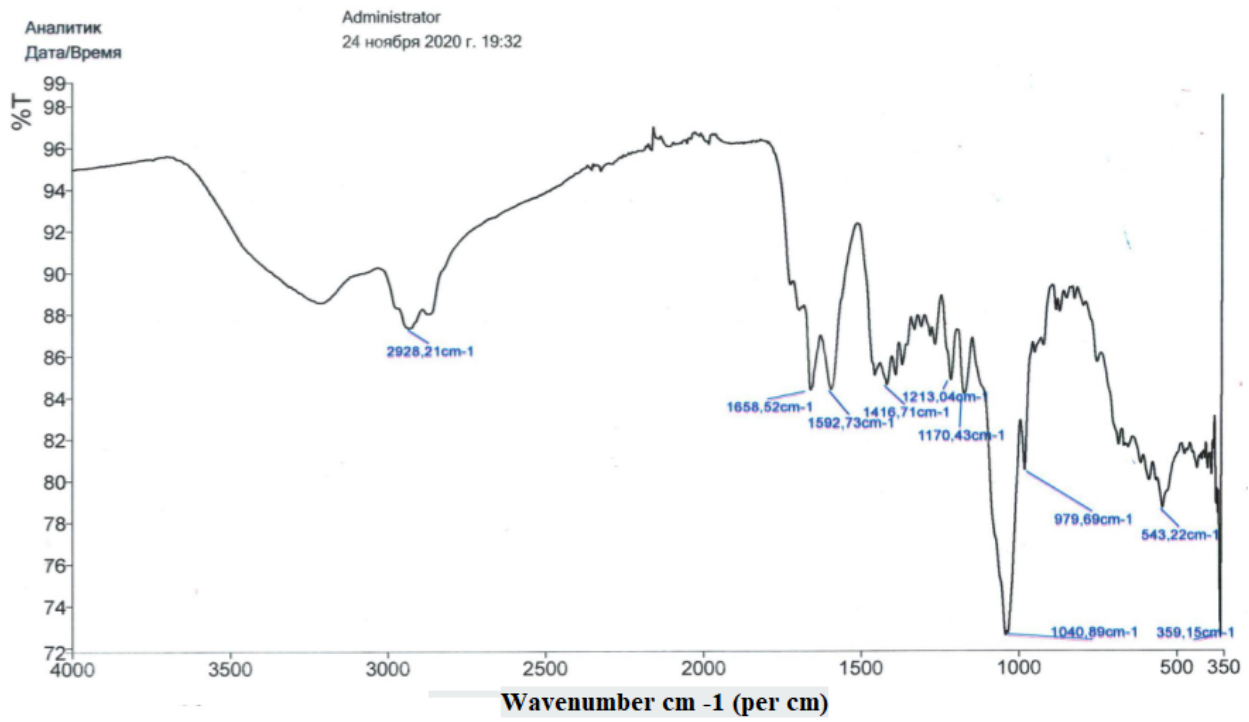

Figure 3 FTIR spectrum of the supramolecular complex GAM:pyrazinamide:isoniazid (4:2:1). The absorption band at 1,658 cm^{-1} corresponds to the C=O stretching vibration of the aglycone, while the intensified band at 1,593 cm^{-1} indicates electrostatic $–COO^{-}\cdots{}^{+}NH_3^{+}$ interactions, confirming supramolecular complex formation.

The observed spectral changes, particularly the shift and intensity variation of the carbonyl and carboxylate bands, demonstrate that the formation of the GAM-pyrazinamide-isoniazid complex involves both hydrogen bonding and electrostatic interactions. These non-covalent forces stabilize the three-dimensional architecture of the supramolecular assembly, which is consistent with the bathochromic shift observed in the UV-Vis spectrum [43].

Molecular docking results

Isoniazid

The molecular docking analysis revealed that isoniazid exhibited moderate binding affinities with the selected immunomodulatory proteins, forming stable non-covalent interactions within their active sites (**Figure 4**). The calculated binding energies were –5.6 kcal/mol for interleukin-6 receptor (1A3Q), –4.6 kcal/mol for interleukin-2 (1VLK), and –5.2 kcal/mol for tumor necrosis factor-α (2AZ5), suggesting favorable but differential binding strengths across the 3 targets.

Interaction with Interleukin-6 Receptor (1A3Q)

In the 1A3Q protein complex, isoniazid was positioned within the hydrophilic pocket surrounded by polar residues. The ligand formed conventional hydrogen bonds with GLN D:125 and VAL B:91, while π-σ and π-alkyl interactions were observed with LEU B:93, contributing to the stabilization of the complex. These multiple interactions indicate that isoniazid can effectively associate with the IL-6R binding site through a combination of hydrogen bonding and hydrophobic stacking effects [32,33].

Interaction with Interleukin-2 (1VLK)

The docking pose of isoniazid within the IL-2 active cavity revealed a hydrogen-bonding network involving ASP A:13 and PHE A:15, together with LEU A:23 and LEU A:105, which stabilized the ligand through van der Waals and π-π interactions. The binding energy of –4.6 kcal/mol indicates a weaker, yet stable association, suggesting that isoniazid may moderately influence IL-2–related immune signaling by partial interaction with its catalytic residues.

Interaction with TNF-α (2AZ5)

In the TNF-α complex, isoniazid formed key hydrogen bonds with DA C:509, DA D:609, and DT D:610, which are located near the DNA-binding interface of the NF-κB subunit (p52-like structural domain). These interactions, along with a slight π-cation contribution, resulted in a binding energy of –5.2 kcal/mol, reflecting a balanced electrostatic and hydrogen-bonding character. The orientation of isoniazid in the TNF-α binding pocket suggests potential modulation of the protein's inflammatory response function.

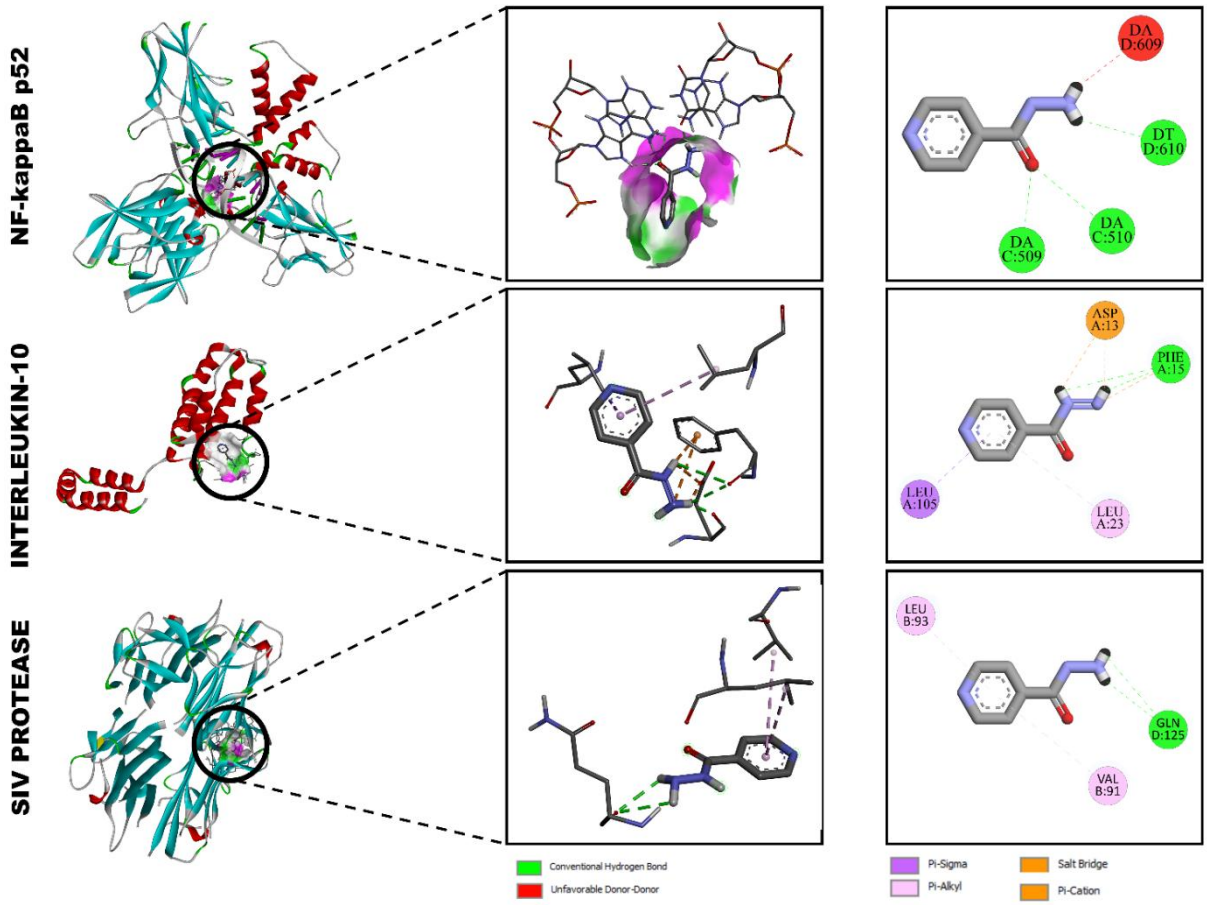

Figure 4 Molecular docking visualization of isoniazid bound to (A) NF-κB p52 (2AZ5), (B) interleukin-2 (1VLK), and (C) interleukin-6 receptor (1A3Q). Green dashed lines indicate hydrogen bonds, violet lines π-interactions, and orange lines salt bridges.

Levofloxacin

Levofloxacin displayed strong binding affinities toward all three immunomodulatory proteins, forming multiple stabilizing interactions in the active cavities (**Figure 5**). The calculated binding energies were –8.8 kcal/mol for interleukin-6 receptor (1A3Q), –6.6 kcal/mol for interleukin-2 (1VLK), and –8.0 kcal/mol for NF-κB p52 (2AZ5), indicating considerably stronger affinity compared with the other ligands studied.

Interaction with interleukin-6 receptor (1A3Q)

Within the IL-6R binding site, levofloxacin formed a network of hydrogen bonds with DG D:608, DA C:510, and LYS B:259, while LYS A:221 participated in an additional salt-bridge interaction. Aromatic stabilization was achieved through π-π stacking and π-σ interactions with TYR A:285. This combination of electrostatic and π-interactions explains the strong binding energy of –8.8 kcal/mol and suggests efficient occupancy of the IL-6R cavity [34,35].

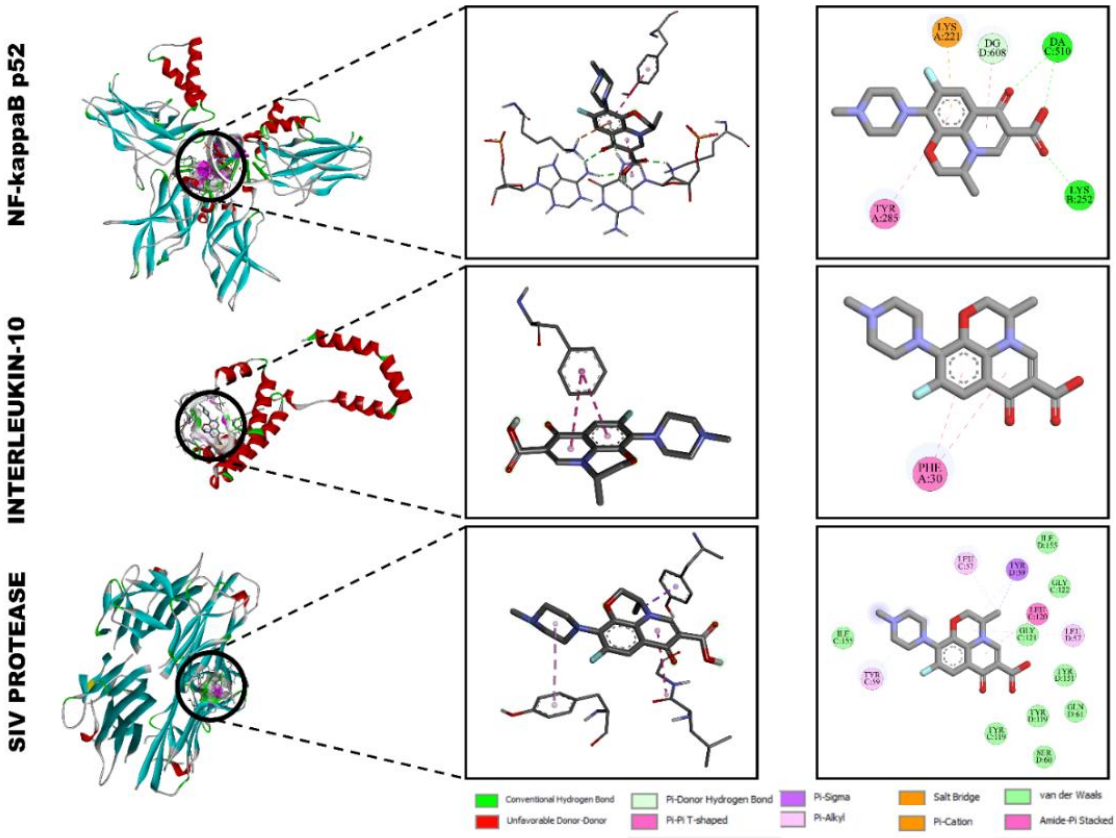

Figure 5 Docking interactions of levofloxacin with (A) NF-κB p52 (2AZ5), (B) interleukin-2 (1VLK), and (C) interleukin-6 receptor (1A3Q).

Interaction with Interleukin-2 (1VLK)

Docking of levofloxacin into IL-2 revealed π-π stacking and π-σ interactions with PHE A:30, supported by van der Waals contacts with nearby hydrophobic residues. The absence of strong polar bonding accounts for the comparatively moderate binding affinity (–6.6 kcal/mol). Nevertheless, these interactions imply potential stabilization of IL-2 through non-polar contacts within its active domain.

Interaction with NF-κB p52 (2AZ5)

In the NF-κB p52 complex, levofloxacin was deeply embedded in the hydrophobic pocket, forming conventional hydrogen bonds with GLN D:381 and TYR B:119, and π-alkyl/ π-π T-shaped interactions with LEU B:157, TYR B:155, and ILE C:135. Additional van der Waals contacts with GLY C:123, GLY C:121, and SER D:160 further stabilized the complex. The cumulative network of polar and aromatic forces yielded a strong binding affinity of –8.0 kcal/mol, suggesting that levofloxacin can efficiently modulate NF-κB signaling by occupying its DNA-binding interface.

Pyrazinamide

The molecular docking study demonstrated that pyrazinamide interacted moderately with all three selected immunomodulatory proteins (**Figure 6**). The obtained binding energies were –5.6 kcal/mol for interleukin-6 receptor (1A3Q), –4.1 kcal/mol for interleukin-2 (1VLK), and –4.5 kcal/mol for NF-κB p52 (2AZ5), reflecting the formation of stable but relatively weak supramolecular associations typical of low-molecular-weight ligands [48,49].

Interaction with interleukin-6 receptor (1A3Q)

In the IL-6 receptor complex, pyrazinamide formed a network of hydrogen bonds with HIS A:90 and ALA A:29, while ARG A:32 participated in a π-π stacking interaction that stabilized the aromatic ring of the ligand. The overall binding geometry positioned pyrazinamide in a polar pocket lined with histidine and alanine residues, supporting its modest but specific affinity (–5.6 kcal/mol). These interactions suggest that pyrazinamide can weakly associate with IL-6R through hydrogen bonding and π-type contacts.

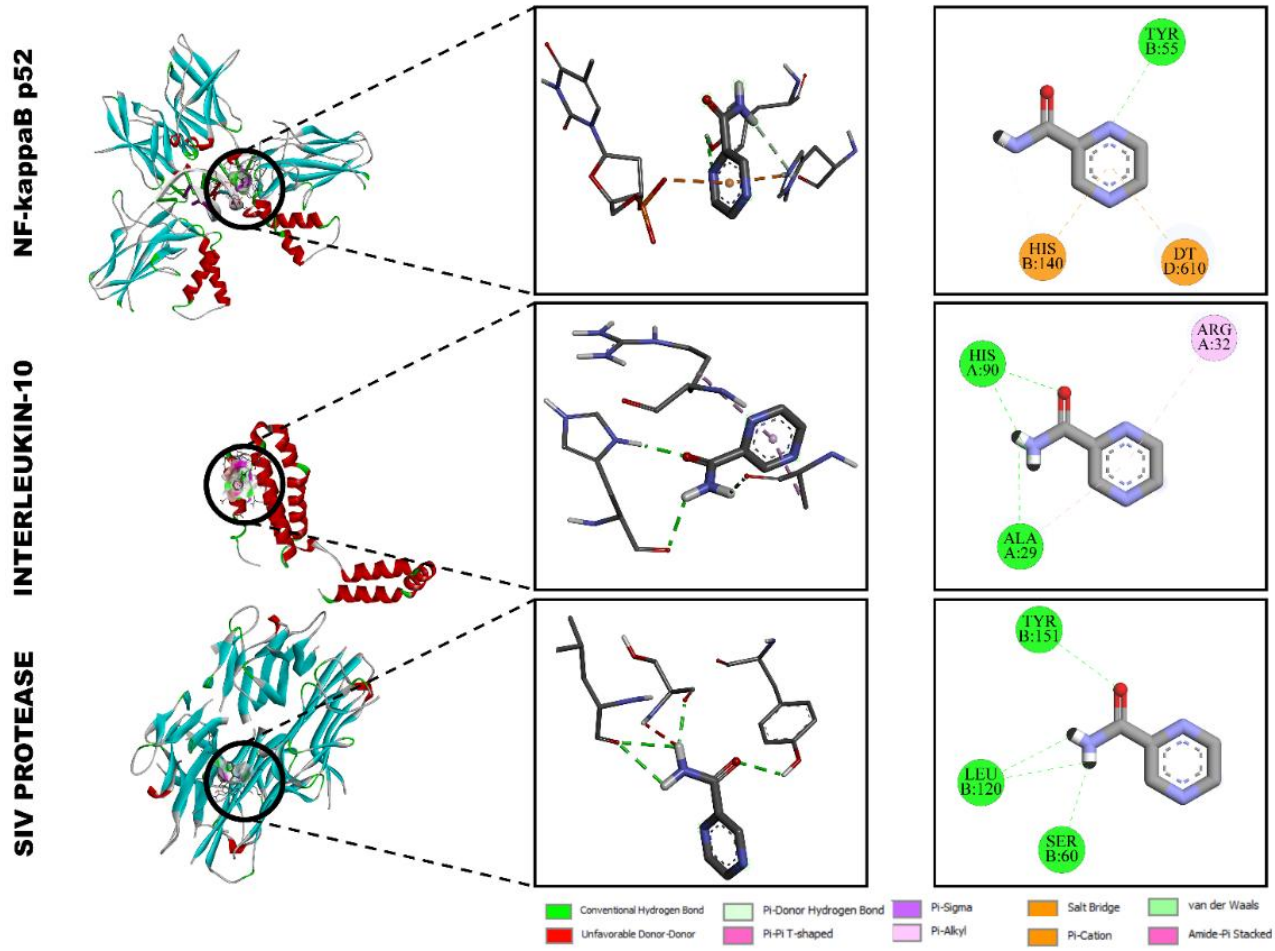

Figure 6 Molecular docking interactions of pyrazinamide with (A) NF-κB p52 (2AZ5), (B) interleukin-2 (1VLK), and (C) interleukin-6 receptor (1A3Q).

Interaction with interleukin-2 (1VLK)

Docking into the IL-2 binding site revealed the presence of π-π T-shaped and π-donor hydrogen bonds between the aromatic moiety of pyrazinamide and the residues PHE A:30 and HIS A:90, with additional weak van der Waals interactions stabilizing the ligand. The relatively low binding energy (–4.1 kcal/mol) corresponds to transient, reversible binding typical of small hydrophilic molecules, indicating limited but potential modulation of IL-2-mediated immune signaling.

Interaction with NF-κB p52 (2AZ5)

In the NF-κB p52 protein complex, pyrazinamide established conventional hydrogen bonds with TYR B:55 and HIS B:140, while DT D:610 contributed to an additional π-cation interaction (–4.5 kcal/mol). The spatial orientation of pyrazinamide within the NF-κB binding pocket placed it close to polar and aromatic residues, suggesting weak electrostatic attraction and partial π-π stabilization.

Rifampicin

The molecular docking results demonstrated that rifampicin showed the strongest binding affinity among all tested molecules toward the selected immunomodulatory proteins (**Figure 7**). The calculated binding energies were –9.2 kcal/mol for NF-κB p52 (2AZ5), –8.8 kcal/mol for interleukin-10 (1VLK), and –8.4 kcal/mol for interleukin-6 receptor (1A3Q). These values indicate a high degree of molecular complementarity and stable non-covalent interactions, reflecting the strong affinity of rifampicin to key immunoregulatory targets [36,37].

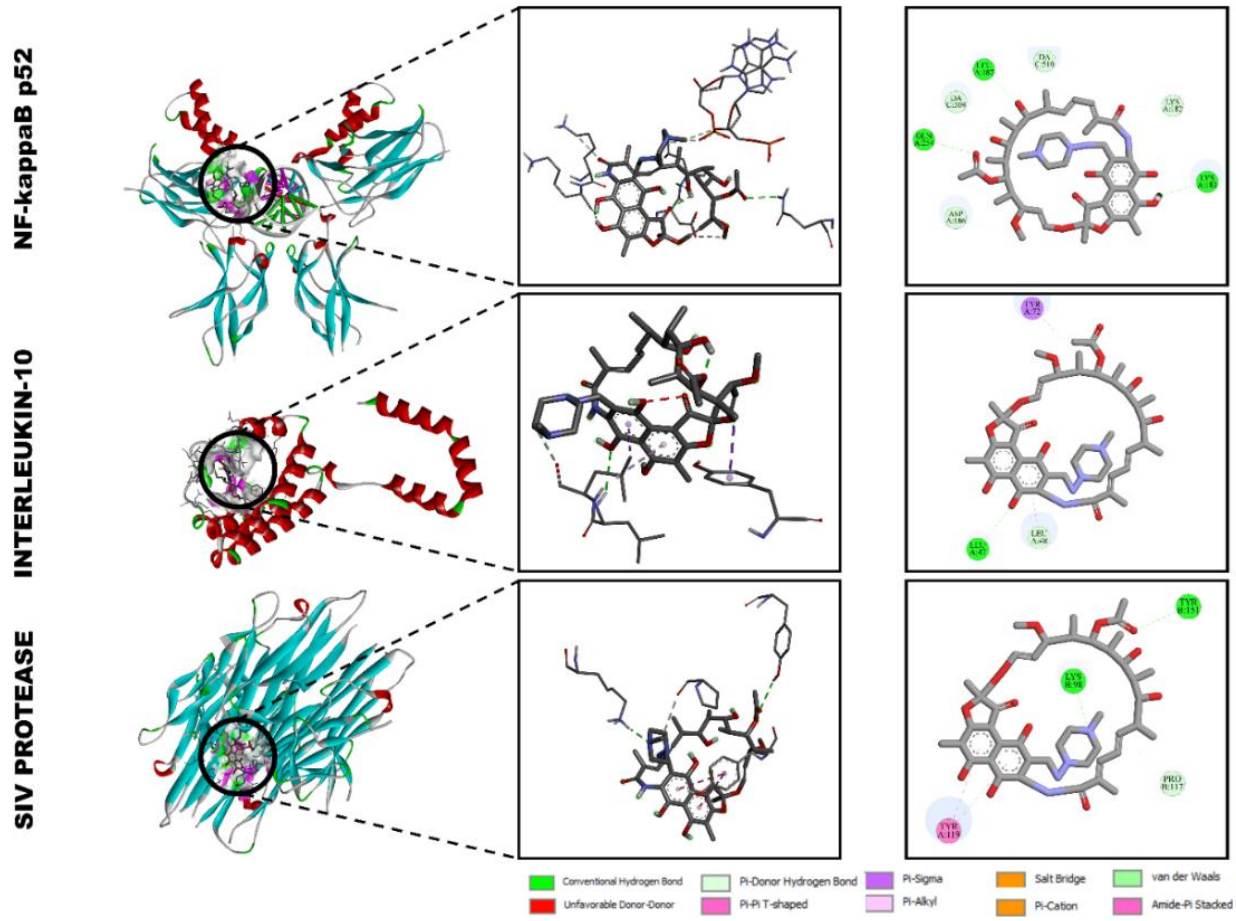

Figure 7 Molecular docking interactions of rifampicin with (A) NF-κB p52 (2AZ5), (B) interleukin-10 (1VLK), and (C) interleukin-6 receptor (1A3Q).

Interaction with NF-κB p52 (2AZ5)

Rifampicin bound tightly within the hydrophobic pocket of NF-κB p52, forming multiple hydrogen bonds with residues ASP A:318, ARG A:319, and LYS A:318, along with π-π T-shaped interactions involving TYR A:118. The carbonyl and hydroxyl groups of rifampicin participated in electrostatic and van der Waals interactions with DA C:509 and LYS A:318, stabilizing the binding pose. These interactions suggest that rifampicin may effectively interfere with the DNA-binding or dimerization domain of NF-κB, which is critical for its transcriptional activity.

Interaction with interleukin-10 (1VLK)

In the IL-10 complex, rifampicin showed strong hydrogen bonding with LEU A:43 and ASP A:13, complemented by π-π stacking interactions with TYR A:15 and PHE A:30. The molecule was stabilized by a network of van der Waals forces involving LEU A:48 and ILE A:37, leading to a total binding energy of –8.8 kcal/mol. This interaction profile implies that rifampicin can occupy the IL-10 receptor pocket, potentially modulating cytokine signaling and anti-inflammatory responses.

Interaction with interleukin-6 receptor (1A3Q)

In the IL-6R docking complex, rifampicin exhibited conventional hydrogen bonds with LYS A:418 and ASP A:418, and π-π stacking with TYR A:419. Additionally, ARG A:318 and DA C:510 formed polar and electrostatic interactions, further stabilizing the ligand orientation (binding energy –8.4 kcal/mol). These multiple non-covalent interactions indicate that rifampicin can interact with residues located near the active cytokine-binding region of IL-6R, supporting its potential immunomodulatory capability.

Acute toxicity assessment of the XF-2 complex

The acute toxicity of the supramolecular complex XF-2 (glycyrrhizic acid monoammonium salt with pyrazinamide, isoniazid, rifampicin, and levofloxacin in a 4:2:1 ratio) was evaluated in white mice according to the classical Litchfield and Wilcoxon probit analysis method (**Table 1**). The experimental animals received the test substance orally in doses ranging from 2,025 to 5,670 mg/kg, with groups of six animals per dose [38,39]. The mortality data were used to determine the median lethal dose (LD_{50}).

Table 1 Results of the study of acute toxicity indices of the XF-2 complexes.

Doses	Number of animals dead/total
2,025 mg/kg	0/6
2,835 mg/kg	1/6
3,645 mg/kg	2/6
4,455 mg/kg	3/6
5,265 mg/kg	5/6
5,670 mg/kg	6/6
LD_{50} = 4,050 (3,375÷4,860) mg/kg	

The calculated LD_{50} value for the XF-2 complex was 4,050 mg/kg (95% confidence limits: 3,375 - 4,860 mg/kg). According to the toxicity classification system proposed by Stefanov (1998), this value places the compound within toxicity class IV - "low-toxic" substances, indicating a high degree of safety for oral administration. Throughout the 14-day observation period, no delayed toxic effects or severe behavioral abnormalities were recorded in surviving animals. The transient signs of mild central nervous system depression (reduced motor activity, short-term drowsiness) observed at higher doses subsided within the first 24 h, suggesting that the nervous system may be the primary target of acute exposure.

Table 2 Calculation of LD50 using the Litchfield and Wilcoxon scheme using probit analysis of the XF2 complex.

Doses	Observed effect	% effect (observed)	% effect (expected)	Difference between observed and expected % effect	The term for X^2
3,405 mg/kg	0/6	0	0	0	0
4,540 mg/kg	1/6	16.6	8	8.6	0.1
5,675 mg/kg	2/6	33.3	36	2.4	0.003
6,810 mg/kg	3/6	50.0	64	14	0.085
7,945 mg/kg	5/6	83.3	82	1.3	0.002
8,512 mg/kg	6/6	96.9	90	6.9	0.05
				Sum	0.24

These results demonstrate that the inclusion of anti-tuberculosis agents into the supramolecular matrix of glycyrrhizic acid does not increase systemic toxicity, confirming the safety and biocompatibility of the supramolecular framework.

Immunomodulatory activity of the XF-2 complex

The immunomodulatory potential of the XF-2 complex was investigated under conditions of prednisolone-induced immunosuppression. The relative weight coefficients of the thymus and spleen were

measured as key indicators of immune organ restoration (**Table 2**). Prednisolone treatment resulted in a marked reduction in the thymus and spleen indices compared with the intact control, confirming the development of immunosuppression. Upon administration of the XF-2 complex at doses of 500, 1,000, and 1,500 mg/kg, a dose-dependent increase in both thymus and spleen indices was observed [40,41]. The most pronounced effect was achieved at 1,000 mg/kg, where the relative weight coefficients reached 0.057 ± 0.006 for the thymus and 0.671 ± 0.067 for the spleen, approaching the levels of intact animals. At lower (500 mg/kg) and higher (1,500 mg/kg) doses, the increase was moderate, indicating a bell-shaped dose-response typical of natural immunomodulators. The obtained data demonstrate that XF-2 effectively counteracts glucocorticoid-induced atrophy of lymphoid organs, suggesting restoration of immune homeostasis. Such effects are consistent with the known immunoprotective and anti-inflammatory mechanisms of glycyrrhizic acid and its derivatives, which are capable of stabilizing cell membranes, modulating cytokine production, and interacting with transcriptional regulators such as NF-κB p52 and interleukin-10 receptors.

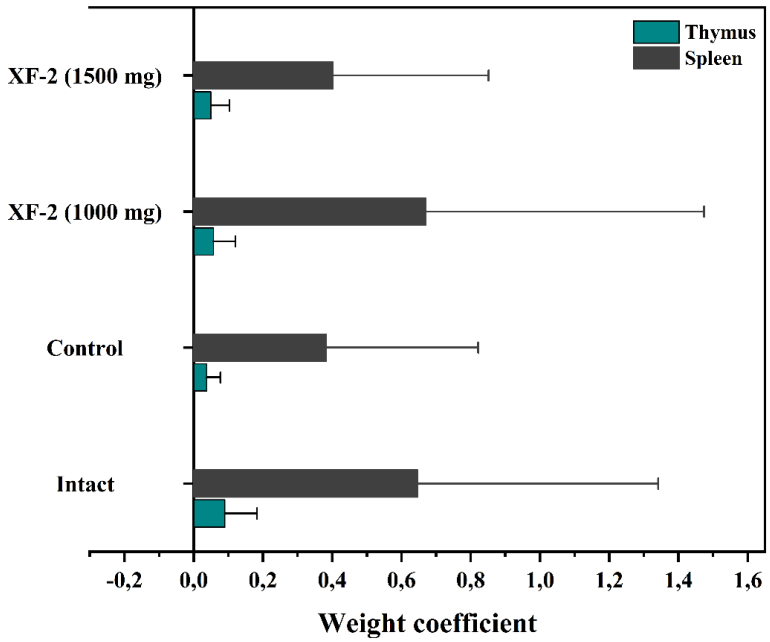

Figure 8 Effect of the supramolecular complex XF-2 on the relative weight coefficients of the thymus and spleen in mice with prednisolone-induced immunosuppression.

The computational docking results further support these findings: Active molecules within the XF-2 complex (isoniazid, pyrazinamide, rifampicin, levofloxacin) displayed strong binding affinities to key immunomodulatory proteins (binding energies ranging from –4.6 to –9.2 kcal/mol), forming stable hydrogen-bonding and π-stacking networks that may contribute to enhanced immunoregulatory signaling.

Discussion

The present study demonstrated that the supramolecular complex XF-2, composed of glycyrrhizic acid monoammonium salt and the anti-tuberculosis drugs pyrazinamide, isoniazid, rifampicin, and levofloxacin, possesses a balanced combination of physicochemical stability, low toxicity, and immunomodulatory potential. Integration of spectroscopic, computational, and *in vivo* data provides a coherent understanding of the mechanisms underlying its biological action.

Spectroscopic evidence of complex formation

The UV-Vis and FTIR analyses confirmed the supramolecular assembly between glycyrrhizic acid monoammonium salt and the incorporated drug molecules. The bathochromic shift in the UV spectrum

from 254 to 264 nm reflected electronic transitions associated with n→π* charge delocalization, indicating the formation of hydrogen-bonded and electrostatically stabilized aggregates.

Similarly, in the FTIR spectrum, the enhancement of the carboxylate band at 1,593 cm^{-1} and the shift of the C=O stretching vibration to 1,658 cm^{-1} verified the involvement of $–COO^{-}\cdots{}^{+}NH_3^{+}$ ionic bridges, characteristic of supramolecular host-guest interactions. These findings highlight that complexation occurs through both hydrogen bonding and electrostatic association, leading to an organized three-dimensional network capable of encapsulating hydrophilic and hydrophobic drug molecules simultaneously.

Molecular docking insights

Computational docking studies further elucidated the potential immunoregulatory targets of the XF-2 components. Among the evaluated proteins—NF-κB p52 (2AZ5), interleukin-10 (1VLK), and interleukin-6 receptor (1A3Q)—rifampicin exhibited the highest binding affinity (–9.2 to –8.4 kcal/mol), followed by levofloxacin (–8.8 to –6.6 kcal/mol), whereas isoniazid and pyrazinamide displayed moderate affinities (–5.6 to –4.1 kcal/mol). These interactions involved key amino acid residues such as ASP, ARG, TYR, and LYS, forming conventional hydrogen bonds, π-π stacking, and electrostatic contacts within the active sites of the immunomodulatory proteins. In particular, rifampicin and levofloxacin showed stable binding near the DNA-binding and receptor-interface regions of NF-κB and IL-10, suggesting that these molecules might suppress pro-inflammatory transcription or modulate cytokine signaling. The combined docking profile of the XF-2 complex implies that the supramolecular encapsulation of these drugs in glycyrrhizic acid may enhance their biostability, target affinity, and immunomodulatory precision through synergistic non-covalent interactions.

In vivo pharmacological findings

In the acute toxicity assay, XF-2 exhibited an LD_{50} of 4,050 mg/kg, corresponding to toxicity class IV ("low-toxic"), confirming its high margin of safety. No severe behavioral changes or delayed toxic effects were observed, indicating good systemic tolerance. The supramolecular architecture of glycyrrhizic acid appears to mitigate the inherent toxicity of individual antituberculosis agents, likely by modulating their absorption rate and biodistribution. Under conditions of prednisolone-induced immunosuppression, administration of the XF-2 complex produced a dose-dependent increase in the relative weight coefficients of the thymus and spleen. The most pronounced recovery was observed at 1,000 mg/kg, where both parameters approximated those of the intact control group. This suggests restoration of thymolymphatic function and splenic immune competence. Such effects are consistent with the well-documented ability of glycyrrhizic acid to activate T-cell differentiation, normalize cytokine balance, and protect lymphoid tissue from glucocorticoid-induced atrophy.

Overall interpretation

Taken together, the results confirm that the formation of supramolecular complexes with glycyrrhizic acid monoammonium salt provides a rational strategy for designing multifunctional drug systems combining safety, bioavailability, and immunomodulatory efficacy. The XF-2 complex, in particular, demonstrates a strong structural-functional correlation between its molecular architecture and biological behavior. Through a combination of hydrogen-bonded encapsulation, electrostatic stabilization, and protein-level targeting, XF-2 enhances immune resilience while maintaining low systemic toxicity. These findings suggest that XF-2 can be considered a promising candidate for further preclinical and pharmacodynamic studies, aimed at developing novel supramolecular immunomodulatory formulations with potential applications in infectious and inflammatory diseases.

Conclusions

The supramolecular complex XF-2, based on glycyrrhizic acid monoammonium salt and the anti-tuberculosis agents pyrazinamide, isoniazid, rifampicin, and levofloxacin, demonstrated a favorable balance between chemical stability, safety, and biological efficacy. Spectroscopic and computational analyses confirmed the formation of a stable hydrogen-bonded and electrostatically coordinated supramolecular structure capable of interacting with key immunoregulatory proteins such as NF-κB p52, IL-10, and IL-6R. *In vivo*, XF-2 exhibited low acute toxicity

(LD_{50} = 4,050 mg/kg) and a pronounced immunomodulatory effect, restoring thymic and splenic indices under prednisolone-induced immunosuppression, with the maximal response observed at 1,000 mg/kg. The obtained results highlight the potential of XF-2 as a safe and multifunctional supramolecular formulation with combined immunorestorative and protective activity, warranting further pharmacodynamic and clinical evaluation.

Acknowledgements

We would like to thank Academy Sciences of the Republic of Uzbekistan.

Declaration of Generative AI in Scientific Writing

Only minimal assistance was used from QuillBot for paraphrasing selected sentences. All scientific content, interpretation, and conclusions were developed independently by the authors.

CRediT Author Statement

Fayyoza Khurramova: Performed the main experimental work, analyzed the data, and prepared the first draft of the manuscript. **Rakhmat Esanov:** Conceived and designed the study, supervised the experimental design and synthesis process, and revised the manuscript critically for important intellectual content. **Izzatullo Abdullaev:** Contributed to biological assays, data validation, and interpretation of pharmacological results. **Ulugbek Gayibov:** Performed statistical analysis, molecular modeling, and contributed to the writing and discussion of the results. **Kuralbay Rezhepov:** Assisted in spectroscopic characterization, data curation, and preparation of graphical materials. **Alimjon Matchanov:** Coordinated the overall research project, provided resources and funding acquisition, and approved the final version of the manuscript.

References

[1] RS Esanov, AZ Dzhuraev, KS Rafikova, Z Khashimova, E Berdibaev, D Abdurazzakova and A Matchanov. Synthesis and biological activity of some esters of glycyrretinic acid. *Engineered Science* 2024; **31**, 1212.

[2] KA Yuldashev, RS Esanov, HT Saidullaeva, VV Uzbekov, MK Salakhutdinova, ZS Khashimova, MB Gafurov, YI Oshchepkova and SI Salikhov. Creation of modified forms of amiodarone with glycyrrhizic acid and its monoammonium salt and study of their cytotoxicity on HeLa cells. *Pharmaceutical Chemistry Journal* 2024; **57**, 1726-1731.

[3] MB Rakhimova, RS Esanov, PG Merzlyak, MB Gafurov, RS Kurbannazarova, OD Matchanov and RZ Sabirov. Effect of glycyrrhetic acid derivatives on regulation of thymocyte volume. *Bulletin of Experimental Biology and Medicine*, 2023; **175(1)**, 27-31.

[4] RS Esanov, KM Bobakulov, ND Abdullaev, MB Gafurov and KA Yuldashev. Synthesis of new 18β-H-glycyrrhetic acid amides with several 2-amino-5-alkylaminothiadiazoles. *Chemistry of Natural Compounds* 2021; **57**, 335-338.

[5] DT Babaeva, RS Esanov, AA Akhunov, MB Gafurov, NR Khashimova and AD Matchanov. Biological activity of the supramolecular complex of glycyrrhizic and salicylic acids. *Chemistry of Natural Compounds*, 2020; **56(2)**, 278-281.

[6] AD Matchanov, DN Dalimov, UN Zainutdinov, NL Vypova, AK Islamov and BM Bekpolatova. Preparation and physicochemical and biological properties of molecular associates of lagochilin and lagochirsine with glycyrrhizic acid and its monoammonium salt. *Chemistry of Natural Compounds* 2020; **53(4)**, 665-669.

[7] AD Matchanov, RS Esanov, T Renkawitz, AB Soliev, E Kunisch, I Gonzalo de Juan, F Westhauser and DU Tulyaganov. Synthesis, structure-property evaluation and biological assessment of supramolecular assemblies of bioactive glass with glycyrrhizic acid and its monoammonium salt. *Materials* 2022; **15(12)**, 4197.

[8] Mamajanov, M., Abdullaev, I., Sotimov, G., Mavlanova, S., Niyozov, Q., Mirzaolimov, M., Najimov, A., Mirzaolimov, E., Raximberganov, M, & Abdullayev, U. Mitochondrial and Pharmacokinetic Insights into 3,5,7,2',6'-Pentahydroxyflavanone: Respiratory Modulation, Calcium Handling, and Membrane Stability. *Trends in Sciences*, 2025; *22***(12)**, 10984.

[9] Aripov, T.F., Gayibov, U.G., Gaibova, S.N. *et al. In Vitro* Antioxidant and Antiradical Activity

of Rutan, a Polyphenolic Extract from the Tannic Sumach (*Rhus coriaria* L.) Leaves. *Russ J Bioorg Chem,* 2025; **51**, 3077–3085

[10] Li, M., Zhang, M., Fatixovich, A.T. *et al.* Green-synthesized Zn^{2+}-polyphenol networks (CGA/RA) for enhanced multifunctional food preservation. *Food Measure* (2025).

[11] Ulugbek G, Izzatullo A, Fotima S, Sirojiddin O, Azizbek A, Sabina G, et al. Plant derived and synthetical antihypoxic agents in cardiovascular diseases: Mechanisms, key pathways and therapeutic potential. Plant Sci. Today. 2025; 12**(4)**.

[12] I Abdullaev, U Gayibov, S Omonturdiev, S Fotima, S Gayibova and T Aripov. Molecular pathways in cardiovascular disease under hypoxia: Mechanisms, biomarkers, and therapeutic targets. *The Journal of Biomedical Research* 2025; **39(3)**, 254-269.

[13] AA Abdullaev, DR Inamjanov, DS Abduazimova, SZ Omonturdiyev, UG Gayibov, SN Gayibova and TF Aripov. *Silybum mariánum*'s impact on physiological alterations and oxidative stress in diabetic rats. *Biomedical and Pharmacology Journal* 2024; **17(2)**, 1291-1300.

[14] AV Mahmudov, OS Abduraimov, SB Erdonov, UG Gayibov and LY Izotova. Bioecological features of *Nigella sativa* L. in different conditions of Uzbekistan. *Plant Science Today* 2022; **9(2)**, 421-426.

[15] AZ Dzhuraev, RS Esanov, AA Ganiev, KM Bobakulov, ND Abdullaev and AD Matchanov. Synthesis of new amides of 3-O-acetyl-18β-H-glycyrrhetic acid. *Chemistry of Natural Compounds* 2024; **60(1)**, 80-83.

[16] AQQ Azimova, AX Islomov, SA Maulyanov, DG Abdugafurova, LU Mahmudov, IZ Abdullaev, AS Ishmuratova, SQQ Siddikova and IR Askarov. Determination of vitamins and pharmacological properties of *Vitis vinifera* L. syrup-honey. *Biomedical and Pharmacology Journal* 2024; **17(4)**, 2779-2786.

[17] AD Matchanov, FN Tashpulatov, FA Sobirova, AV Filatova, RS Esanov, KV Raimova and NL Vypova. Hemostatic activity of "Glilagel" gel based on lagochilin with monoammonium salt of glycyrrhizic acid. *Experimental and Clinical Pharmacology* 2020; **83(11)**, S20-S22.

[18] E Pashkina, V Evseenko, N Dumchenko, M Zelikman, A Aktanova, M Bykova, M Khvostov, A Dushkin and V Kozlov. Preparation and characterization of a glycyrrhizic acid-based drug delivery system for allergen-specific immunotherapy. *Nanomaterials* 2021; **12(1)**, 148.

[19] YG Sıdır and I Sıdır. Optical properties, UV-Vis absorption and fluorescence spectra of 4-pentylphenyl 4-n-benzoate derivatives in different solvents. *Journal of Fluorescence* 2025; **12(1)**, 148.

[20] O Gaibullayeva, A Islomov, D Abdugafurova, B Elmurodov, B Mirsalixov, L Mahmudov, I Abdullaev, K Baratov, S Omonturdiev and S Sa'dullayeva. *Inula helenium* L. root extract in sunflower oil: Determination of water-soluble vitamins and immunity-promoting effect. *Biomedical and Pharmacology Journal* 2024; **17(4)**, 2729-2737.

[21] A Abdullaev, I Abdullaev, A Bogbekov, U Gayibov, S Omonturdiev, S Gayibova, M Turahodjayev, K Ruziboev and T Aripov. Antioxidant potential of *Rhodiola heterodonta* extract: Activation of Nrf2 pathway via integrative *in vivo* and *in silico* studies. *Trends in Sciences* 2025; **22(5)**, 9521.

[22] OS Zoirovich, AIZ Ugli, ID Raxmatillayevich, ML Umarjonovich, ZM Ravshanovna and G Sabina. The effect of *Ajuga turkestanica* on the rat aortic smooth muscle ion channels. *Biomedical and Pharmacology Journal* 2024; **17(2)**, 1213-1222.

[23] D Inomjonov, I Abdullaev, S Omonturdiev, A Abdullaev, L Maxmudov, M Zaripova, M Abdullayeva, D Abduazimova, S Menglieva, S Gayibova, M Sadbarxon, U Gayibov and T Aripov. *In vitro* and *in vivo* studies of *Crataegus* and *Inula helenium* extracts: Their effects on rat blood pressure. *Trends in Sciences* 2025; **22(3)**, 9158.

[24] S Sodiqova, S Kadirova, A Zaynabiddinov, I Abdullaev, L Makhmudov, U Gayibov, M Yuldasheva, M Xolmirzayeva, R Rakhimov, A Mutalibov and H Karimjonov. Channelopathy activity of A-41 (propyl ester of gallic acid):

Experimental and computational study of antihypertensive activity. *Trends in Sciences* 2025; **22(9)**, 10496.

[25] R Sayidaliyeva, S Kadirova, A Zaynabiddinov, I Abdullaev, L Makhmudov, U Gayibov, M Yuldasheva, M Kholmirzayeva, R Rakhimov, A Mutalibov and H Karimjonov. A-51 as a natural calcium channel blocker: An integrative study targeting hypertension. *Trends in Sciences* 2025; **22(11)**, 10760.

[26] A Khasanov, I Abdullaev, S Kadirova, M Mamajanov, A Zaynabiddinov, S Omonturdiev, L Makhmudov, D Inomjonov, U Gayibov, R Esanov and A Matchanov. N-2 polyphenol targets vascular calcium channels to exert antihypertensive effects: *In vitro* and *in vivo* evaluation. *Trends in Sciences* 2025; **22(12)**, 10782.

[27] O Trott and AJ Olson. AutoDock Vina: Improving the speed and accuracy of docking with a new scoring function, efficient optimization, and multithreading. *Journal of Computational Chemistry* 2010; **31(2)**, 455-461.

[28] M Zaripova, I Abdullaev, A Bogbekov, U Gayibov, S Omonturdiev, R Makhmudov, N Ergashev, G Jabbarova, S Gayibova and T Aripov. *In vitro* and *in silico* studies of *Gnaphalium uliginosum* extract: Inhibition of α-amylase and α-glucosidase as a potential strategy for metabolic syndrome regulation. *Trends in Sciences* 2025; **22(8)**, 10098.

[29] UG Gayibov, SN Gayibova, DS Abduazimova, RN Rakhimov, HS Ruziboev, MA Xolmirzayeva, AE Zaynabiddinov and TF Aripov. Antioxidant and cardioprotective properties of polyphenolic plant extract of *Rhus glabra* L. *Plant Science Today* 2024; **11(3)**, 2348-1900.

[30] TF Aripov and UG Gayibov. Antiradical and antioxidant activity of the preparation “Rutan” from *Rhus coriaria* L. *Journal of Theoretical and Clinical Medicine* 2023; **4**, 164-170.

[31] MR Zaripova, SN Gayibova, RR Makhmudov, AA Mamadrahimov, NL Vypova, UG Gayibov, SM Miralimova and TF Aripov. Characterization of *Rhodiola heterodonta* (Crassulaceae): Phytocomposition, antioxidant and antihyperglycemic activities. *Preventive Nutrition and Food Science* 2024; **29(2)**, 135-145.

[32] AV Mahmudov, OS Abduraimov, SB Erdonov, AL Allamurotov, OT Mamatkasimov, UG Gayibov and LY Izotova. Seed productivity of *Linum usitatissimum* L. in different ecological conditions of Uzbekistan. *Plant Science Today* 2022; **9(4)**, 1090-1101.

[33] A Sandoo, JJCSV van Zanten, GS Metsios, D Carroll and GD Kitas. The endothelium and its role in regulating vascular tone. *The Open Cardiovascular Medicine Journal* 2010; **4**, 302-312.

[34] TF Aripov, UG Gayibov, SN Gaibova, YI Oshchepkova and SI Salikhov. *In vitro* antioxidant and antiradical activity of the total polyphenols of *Rhus coriaria* L. leaves (substances of the antiviral drug “Rutan”). *Khimiya Rastitel’nogo Syr’ya* 2024; **4**, 138-148.

[35] UG Gayibov, EJ Komilov, RN Rakhimov, NA Ergashev, NG Abdullajanova, MI Asrorov and TF Aripov. Influence of a new polyphenol compound from Euphorbia plant on mitochondrial function. *Journal of Microbiology, Biotechnology and Food Sciences* 2019; **8(4)**, 1021-1025.

[36] Y Umidakhon, B Erkin, G Ulugbek, N Bahadir and A Karim. Correction of mitochondrial NADH oxidase activity, peroxidation and phospholipid metabolism by haplogenin-7-glucoside in hypoxia and ischemia. *Trends in Sciences* 2022; **19(21)**, 6260.

[37] MK Pozilov, U Gayibov, MI Asrarov, NG Abdulladjanova, HS Ruziboev and TF Aripov. Physiological alterations of mitochondria under diabetes condition and its correction by polyphenol gossitan. *Journal of Microbiology, Biotechnology and Food Sciences* 2022; **12(2)**, 2224.

[38] AG Vakhobjonovna, KE Jurayevich, AIZ Ogli, EN Azamovich, MR Rasuljonovich and AM Islomovich. Tannins as modulators in the prevention of mitochondrial dysfunction. *Trends in Sciences* 2025; **22(8)**, 10436.

[39] Z Shakiryanova, R Khegay, U Gayibov, A Saparbekova, Z Konarbayeva, A Latif and O Smirnova. Isolation and study of a bioactive extract enriched with anthocyanin from red grape

pomace (Cabernet Sauvignon). *Agronomy Research* 2023; **21(3)**, 1293-1303.

[40] U Gayibov, SN Gayibova, KP Ma'murjon, FS Tuxtaeva, UR Yusupova, GMK Djabbarova, ZA Mamatova, NA Ergashev and TF Aripov. Influence of quercetin and dihydroquercetin on some functional parameters of rat liver mitochondria. *Journal of Microbiology, Biotechnology and Food Sciences* 2021; **11(1)**, e2924.